Analysis of the mutually perturbed $(3^1\Pi_u, 4^1\Pi_u) \leftarrow X^1\Sigma_g^+$ band system in Li₂

ZBIGNIEW JĘDRZEJEWSKI-SZMEK[1*], ANNA GROCHOLA[1],
WŁODZIMIERZ JASTRZĘBSKI[2], PAWEŁ KOWALCZYK[1]

[1]Institute of Experimental Physics, University of Warsaw, ul. Hoża 69, 00-681 Warszawa, Poland

[2]Institute of Physics, Polish Academy of Sciences, ul. Lotników 32/46, 02-668 Warszawa, Poland

*Corresponding author: Zbigniew.Jedrzejewski-Szmek@fuw.edu.pl

Excitation spectra of the $3^1\Pi_u$ and $4^1\Pi_u$ states of the $^7\text{Li}_2$ lithium dimer were measured. Polarization labelling spectroscopy was used to limit visible transitions to one or a few vibrational progressions. Positions of the observed spectra are consistent with previous measurements, but the assignment of quantum numbers to transitions is new. Adiabatic potentials were constructed, and the rovibrational levels were found to be perturbed by nearby Σ states, but also by interaction between both Π states. Deperturbation analysis was attempted by extending the IPA method with a simultaneous treatment of two electronic states. Results of the deperturbation procedure are yet not fully satisfactory, but it is hoped that together with improved adiabatic potentials they will account for the positions of the observed energy levels.

Keywords: diatomic molecules, polarization labelling spectroscopy, inverted perturbation approach.

1. Introduction

Lithium dimer is the lightest homonuclear molecule with core electrons, relatively easy to investigate both experimentally and through numerical computations. In this article we characterize experimentally two electronic states of $^1\Pi_u$ symmetry in this molecule, located $34000-40000$ cm^{-1} above the minimum of the ground state $X^1\Sigma_g^+$: the $3^1\Pi_u$ and $4(D)^1\Pi_u$ states. Because of their proximity and similar shapes of the potential curves, the rovibrational levels of both states lie close together and are subject to mutual perturbations.

The $3^1\Pi_u$ and $4^1\Pi_u$ states have been investigated experimentally and theoretically before, but no definite description of them has been published yet. MERCIER *et al.* [1] were the first to observe transitions from the ground state to presumably two adjacent vibrational levels in the $4^1\Pi_u$ state, but were unable to assign their absolute numbering. Subsequently, most of the experimental and theoretical work came from groups located at the University of Kaiserslautern. Spies calculated *ab initio* potential energy curves

for several electronic states in $^7Li_2$, including $3^1\Pi_u$ and $4^1\Pi_u$ [2]. THEISS *et al.* [3] performed high-resolution measurements of fragments of the $3^1\Pi_u \leftarrow X^1\Sigma_g^+$ and $4^1\Pi_u \leftarrow X^1\Sigma_g^+$ systems and were able to characterize the observed vibrational levels using separate sets of molecular constants for each level [3]. Du, Krämer, Manohar, Genter, Karbach and Demtröder refined those measurements by increasing the range of rotational quantum numbers [4]. Weyh, Lokai and Demtröder performed lifetime measurements for selected vibrational levels of both excited states [5] and reported quantitative agreement with new *ab initio* calculations by Henn and Meyer [6]. Regrettably, the references [2, 4, 6] are only available in paper form at the University of Kaiserslautern. In recent years Jasik and Sienkiewicz performed independent calculations of potential energy curves of $^7Li_2$ [7, 8] which provide the most reliable theoretical results to date. We used them extensively to interpret our experimental results.

2. Experiment

2.1. Experimental setup

We use a setup typical for polarization labelling spectroscopy, described in detail in our previous papers [9, 10]. Lithium in the natural isotopic composition is contained in a heat-pipe cell operated at 1000 K with 5 mbar of helium as a buffer gas. A probe laser beam (originating from either an Ar^+–Kr^+ cw laser or a self-constructed dye-laser tuned to a known rovibrational transition in the $A \leftarrow X$ or $B \leftarrow X$ systems of Li_2) and a pump laser beam (UV light from an OPO/OPA system, Sunlite Ex, Continuum, provided with a frequency doubler) pass at a small angle through the cell. Both the OPO and dye-laser are pumped by the third harmonic of an injection seeded Nd:YAG laser (Powerlite 8000). The cell is placed between two crossed polarizers and the probe light is transmitted through them only when a V-type resonance occurs, *i.e.*, frequencies of the laser beams are simultaneously in resonance with transitions originating from the same level in the ground X state. By tuning the frequency of the pump light and monitoring the probe beam transmitted through the crossed polarizers we record a spectrum corresponding to transitions from a known (labelled) level (v'', J'') in the ground state to levels in the two excited states under consideration, $3^1\Pi_u$ and $4^1\Pi_u$.

As the energies of ground state levels are known with high precision [11] we may easily convert the measured transition frequencies to term values of rovibrational levels in the excited states. They serve as the input data for construction of molecular potentials of the $3^1\Pi_u$ and $4^1\Pi_u$ states, which is the final goal of our analysis.

2.2. Experimental uncertainty

The experimental uncertainty of the term values, assuming a correct assignment of the v', J' quantum numbers to them, is comprised of uncertainties in calibration of the spectra (about 0.05 cm^{-1}) and in determination of the centres of the spectral lines (about 0.01 cm^{-1}). The calibration of the spectra is based on simultaneous recording
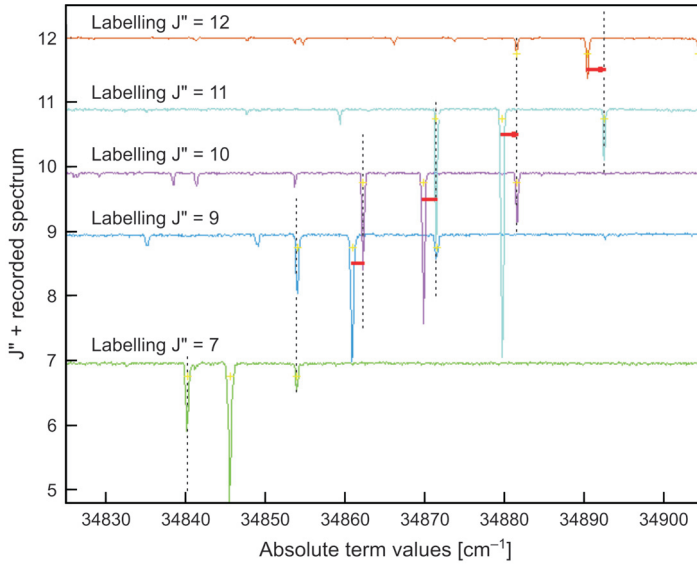
Fig. 1. Verification of an assignment of P and R lines in the spectra. Excitation spectra are shifted by the energy of the ground state (labelled) levels so that positions of the lines correspond to absolute energies of the levels in the upper state. Positions of P and R lines are marked by vertical dashed lines to emphasize the fact that positions of upper levels in transitions observed via R line $(v', J) \leftarrow (v'', J-1)$ and via P line $(v', J) \leftarrow (v'', J'+1)$ are equal. Transitions via Q lines excite levels of different parity and their positions do not coincide with that corresponding to P and R lines (the offset is marked by red arrows), because of the lambda doubling and possible perturbation of levels. Nevertheless, ensuring that the P and R transitions (e parity levels) are assigned correctly gives a proof for an assignment of Q transitions (f parity levels).

of the optogalvanic spectrum of argon and transmission fringes of the Fabry–Pérot air interferometer with a free spectral range equal to 1 cm^{-1}. The calibration process is automated with the help of dedicated software [12]. The final uncertainty is about 0.07 cm^{-1}, which can be verified through observation of transitions to levels with given (v', J', parity) combinations from two different labelled levels in the ground state (see Fig. 1).

3. Analysis

We investigated ${}^7\text{Li}_2$, the most abundant isotopologue of lithium in the natural composition. A total of 414 transitions have been identified, providing energies of 65 levels of the f parity in each of the investigated $3\,{}^1\Pi_u$ and $4\,{}^1\Pi_u$ states. Our measurements cover a large range of v', and thus a large energy range, but only 11 different values of J' ranging from 4 to 47. Therefore, we have augmented our data set with the results of previous experiments. Reference [1] quotes 87 transition frequencies and the experimental uncertainty is not given explicitly, however by comparison with our measurements, it can be estimated as 0.07 cm^{-1}. Reference [3]
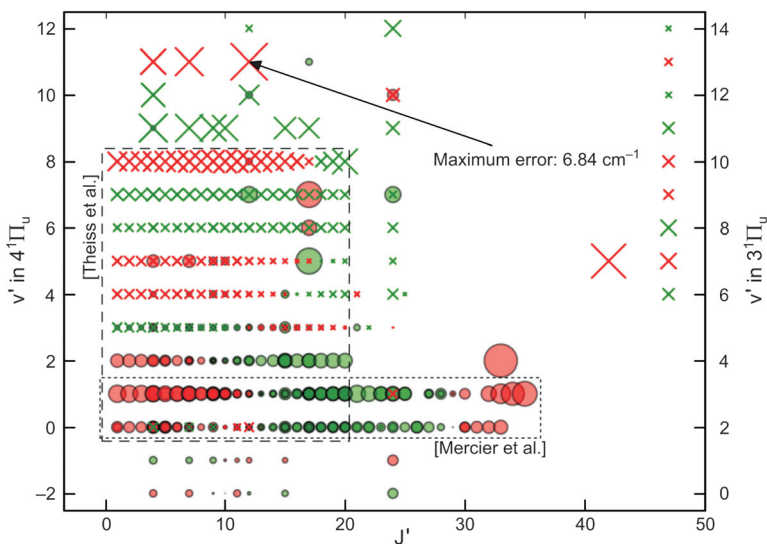
Fig. 2. The span of vibrational and rotational quantum numbers in the data sets corresponding to the *f* parity levels in the $3^1\Pi_u$ and $4^1\Pi_u$ states. In this figure each level is marked with a circle (for $3^1\Pi_u$) or a cross (for $4^1\Pi_u$) with the area proportional to the discrepancy between the experimental energy and the value calculated from the constructed potential energy curves, red for a positive, green for a negative difference. Ranges of quantum numbers covered by MERCIER *et al.* [1] and THEISS *et al.* [3] are surrounded with dashed and dotted lines.

provides coefficients describing energies of *ca.* 200 rovibrational levels accurate to about $0.1-0.3$ cm^{-1}, depending on *v'*. Reference [5] provides energies of only 15 levels, but they are of particular importance because of high *J'* values. The experimental uncertainty is not quoted, but because this is a continuation of measurements from Reference [3], the uncertainty can be assumed to be not worse than 0.1 cm^{-1}. The energies of all levels found in more than one source agree to within 0.26 cm^{-1} (which imposes larger error on experimental uncertainty than 0.07 cm^{-1} of our own measurements). As a result, we had at our disposal energies of 160 and 146 rovibrational levels of f parity in the $3^1\Pi_u$ and $4^1\Pi_u$, respectively (see the identification of lines below). Subsequent optimizations are weighted by the known and estimated uncertainties. The quantum numbers covered by the data are shown in Fig. 2.

3.1. Assignment of observed levels to the two states

From previous measurements and *ab initio* calculations it is known that the shapes of the two potentials are similar and, beginning from the very bottom of the $4^1\Pi_u$ state and *v'* = 2 level in the $3^1\Pi_u$ state, pairs of levels in the two states lie close together. Therefore, also the observed spectral lines are close and there is no easy way to assign the transitions to either of the two excited states. In particular, in [1, 3, 5] the strongest transitions to levels close to the bottom of the $4^1\Pi_u$ state were arbitrarily assigned as transitions to this state, and not to the $3^1\Pi_u$ state. We propose a different assignment

T a b l e. Proposed reassignment of the observed levels.

Identification		Rotationless limit: energy of the level $J' = 1$ [cm^{-1}]	
THEISS *et al*. [3]	This work	Calculated from v'-wise formulas of THEISS *et al*. [3]	This work, energies of solutions calculated from adiabatic potentials
$4^1\Pi_u\ v' = 0$	$3^1\Pi_u\ v' = 2$	34619.6	34619.9
$4^1\Pi_u\ v' = 1$	$3^1\Pi_u\ v' = 3$	34821.2	34821.9
$4^1\Pi_u\ v' = 2$	$3^1\Pi_u\ v' = 4$	35025.3	35025.7
$4^1\Pi_u\ v' = 3$	$3^1\Pi_u\ v' = 5$	35230.0	35229.9
$4^1\Pi_u\ v' = 5$	$4^1\Pi_u\ v' = 3$	35260.6	35260.1
$4^1\Pi_u\ v' = 6$	$4^1\Pi_u\ v' = 4$	35464.6	35465.1
$4^1\Pi_u\ v' = 7$	$4^1\Pi_u\ v' = 5$	35673.6	35674.1
$4^1\Pi_u\ v' = 8$	$4^1\Pi_u\ v' = 6$	35883.6	35883.3
$4^1\Pi_u\ v' = 9$	$4^1\Pi_u\ v' = 7$	36092.2	36091.4
$4^1\Pi_u\ v' = 10$	$4^1\Pi_u\ v' = 8$	36295.6	36297.4

of the observed spectral lines (*cf*. the Table). This new assignment is in agreement with spectral simulations employing the *ab initio* potentials given by JASIK and SIENKIEWICZ [8]. Although the absolute energies given in [8] are off by $70-80$ cm^{-1} when compared to the observed transitions, the predicted separation of vibrational levels in the $3^1\Pi_u$ and $4^1\Pi_u$ states is in reasonable agreement with the experimental data and allows unambiguous identification of transitions. If we shift the *ab initio* potential curves to match the strongest transitions in the observed spectra, several other transitions also fall into place.

Another justification for our novel assignment of transitions is based on comparison of the observed line intensities with the Franck–Condon factors calculated from theoretical potentials. Although in our experimental setup we cannot measure the transition intensity with high precision [13], the observed transition intensities should be in rough agreement with the calculated Franck–Condon factors. In particular, for transitions starting from the labelled $v'' = 0$ level in the ground state, we expect to observe transition intensity slowly growing and then falling, and not with a maximum at $v' = 0$ (*cf*. Fig. 3).

3.2. Perturbation by the Σ states

Apart from the transitions to the two investigated states, we also observe some transitions to nearby states of different symmetry, $3^1\Sigma_u^+$ and $4^1\Sigma_u^+$. Those states contain only levels of *e* parity, in contrast to the Π states which contain levels of *e* and *f* parity. Since the transition rules require a change of parity for the *Q* lines, but forbid it for *P* and *R*, a $\Sigma \leftarrow \Sigma$ spectrum contains only doublets of *P* and *R* lines in vibrational progressions. On the other hand, progressions in $\Pi \leftarrow \Sigma$ spectra consist of *P*, *Q*, *R* triplets, with the strongest *Q* lines leading to levels of *f* parity in the excited state. When we construct a potential based on the *f* levels, the predicted positions of *P* and *R* lines are in agreement with the experimental spectrum for most of the transitions,
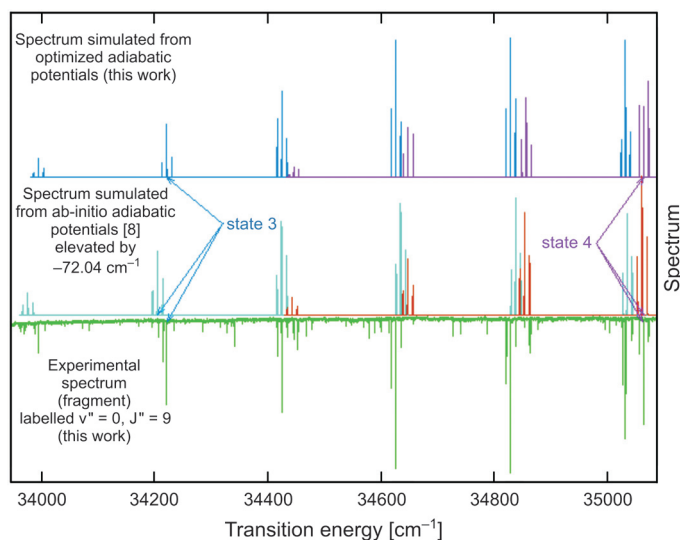
Fig. 3. Comparison of measured and simulated spectra from *ab initio* potentials from [8] (shifted by -72.04 cm^{-1} to align the strong Q transition to $3^1\Pi_u$, $v' = 2$) and our potentials after optimization with the IPA method. The *ab initio* potentials show some disagreement for the two lowest states in $3^1\Pi_u$ and for levels close to $v' = 1, 2$ in $4^1\Pi_u$, and for high levels in both states ($v' > 10$, not shown), but the correspondence with the measured spectrum is clear. In particular, in disagreement with simulated spectra, transitions to $4^1\Pi_u$, $v' = 1$ are not visible. This is probably one of the reasons for previous confusion regarding the identification of transitions.

but for some levels show deviations of at least a few cm^{-1} (even in the region of low J' where the predicted positions of Q lines are very accurate). Most likely this is caused by an interaction of levels of e parity in the Π states with levels of the same parity in the Σ states. Those are local perturbations and their explanation would require a precise knowledge of the potential curves of all states involved. Therefore, at present, we use P and R lines only for identification of transitions (see Fig. 1), without trying to construct potential curves which would precisely reproduce their positions, and the following analysis is based on measured positions of f levels only.

3.3. Adiabatic potential optimization

Levels of the f parity, and thus the observed Q lines, are immune to perturbations by the Σ states. If the assignment of quantum numbers to the observed transitions is unambiguous, construction of a potential curve describing the excited electronic state should be straightforward, provided that enough transitions are recorded.

We applied the inverted perturbation approach (IPA) method [14, and references therein] to construct potentials which reproduce the observed spectral lines. The IPA method is based on minimizing the sum of squares of differences between the measured level energies and those calculated as eigensolutions for a given potential curve. We use a version of the IPA procedure where the potential is defined as a series of points through which smooth cubic splines are drawn ("pointwise IPA" [14]). The first

derivative of the energies of the solutions over the vertical positions of points defining this potential is easily calculated and can be used to "guess" the positions minimizing the average deviation. This linear approximation is not strictly true, so the optimization step has to be repeated a few times.

Using the IPA method two independent potential energy curves were constructed for the $3\,^1\Pi_u$ and $4\,^1\Pi_u$ states, using as a starting point the theoretical potential curves from [8]. The deviation between the observed and calculated energies is shown in Fig. 2. Normally, we would expect the numerical solutions to fit the observed energies within the experimental accuracy (0.07 cm^{-1}, *cf.* Sec. 2.1)[*]. In the present case, however, the smallest rms of deviations which can be achieved with a relatively smooth potential is 0.4 cm^{-1} for $3\,^1\Pi_u$ and 1.3 cm^{-1} for $4\,^1\Pi_u$. One can notice that although the sign of the deviation may change between adjacent v', within a given vibrational level, the deviations change slowly and go smoothly through the zero value (Fig. 2). This is in sharp contrast with a behaviour expected for local rotational perturbations, which in particular are characterized by an abrupt change of sign of the deviation in the vicinity of the perturbation maximum. This behaviour could be explained by the presence of a perturbation of different (non-local) nature.

3.4. Electrostatic perturbations and an extension of the IPA method

The inability to construct adiabatic potentials reproducing observed levels can be attributed to the violation of the adiabatic approximation mixing of eigenfunctions in the two investigated states. LEFEBVRE-BRION and FIELD [15, Chapter 3.3] show that the perturbation of states of the same symmetry in the adiabatic representation is caused by the neglect of the nuclear kinetic energy operator. To find real energies, starting from the adiabatic solutions, one must calculate the off-diagonal matrix elements of the operator mentioned above and diagonalize the full Hamiltonian matrix. This would require a knowledge of both the electronic and rovibrational functions. Fortunately, as shown in [15], one can use the centroid approximation to derive a simplified version of the off-diagonal operator. The effect of the nuclear kinetic energy operator on the electronic wavefunctions is substituted with a two-parameter Lorentzian operator

$$H_{3,\,v_3\sim4,\,v_4} \;=\; -\frac{\hbar}{2\mu}\,\langle\,\xi_{v_3}^{ad}\,\Big|\,\frac{\partial W^e}{\partial R} + 2W^e\frac{\partial}{\partial R}\,\Big|\,\xi_{v_4}^{ad}\,\rangle \tag{1}$$

where ξ^{ad} are the rovibrational functions and

$$W^e(R) \;=\; \frac{H^e/a}{4(H^e/a)^2 + (R - R_C)^2}$$

The parameters H^e, a and R_C are defined through the diabatic solutions of the same molecular Hamiltonian: R_C is the crossing point of diabatic potentials and H^e is

---

[*]The effects of a similar procedure are described in [9, Sec. 3.1].

the diabatic coupling matrix element. Parameter *a* is the tangent of the crossing angle of the diabatic potentials. We can treat H^e/a and R_C as two unknowns to be fitted numerically.

Using this simplified version of the nuclear kinetic energy operator we must calculate the off-diagonal elements for all interacting levels and then diagonalize the resulting matrix. Final eigenfunctions are combinations of solutions from the two potentials and are connected to one or the other state only through the nominal labelling. This procedure is complicated by the fact that this type of perturbation is non-local and actually all vibrational levels with the same rotational quantum number J' interact. Thus all eigenfunctions for a given J' must be found in both potentials and a complete matrix has to be diagonalized. This is not only expensive computationally, but also causes a dependence of the solutions in the region where the transitions have been observed on levels lying far away, outside of the range covered by the experimental data.

We have developed a method of optimizing both potentials and the two parameters defining the perturbation at the same time. The dependence of the diagonalized eigenvalues on the original eigenvalues can be approximated by the first derivative, which is defined through the eigenvectors of the Hamiltonian matrix which we calculate during the diagonalization process. Likewise, the derivative of the simplified nuclear kinetic energy operator from Eq. (1) over the perturbation parameters can be calculated analytically. The availability of derivatives over all parameters means that once we calculate the diagonalized eigenvalues numerically, we also obtain the value of their derivative over the original unperturbed adiabatic eigenvalues and the parameters defining the perturbation. This can be combined with the derivative of energies
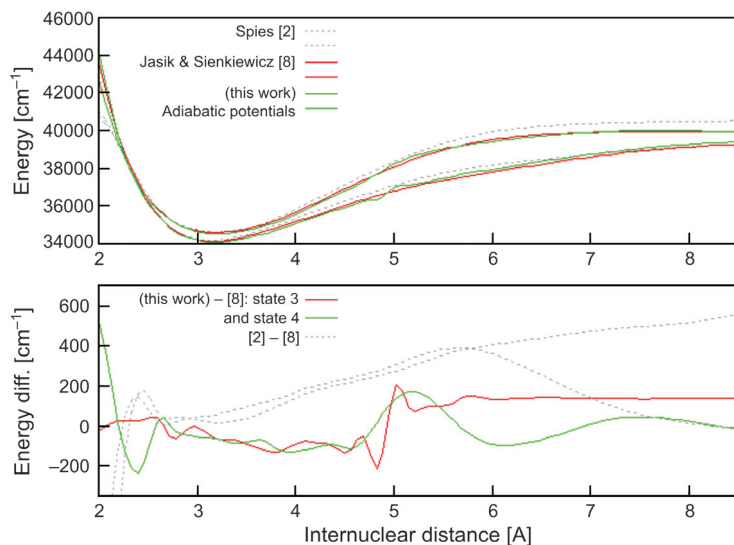

Fig. 4. Comparison of *ab initio* adiabatic potential curves from Spies [2], Jasik and Sienkiewicz [8] and this work.

of adiabatic solutions over the points defining the potential to obtain the dependence of the final eigenvalues on the original potentials and the two extra parameters. This is an extension of the pointwise-IPA to the case of two potentials and two extra parameters, H^e/a and R_C. The vector of deviations to minimize is twice as big and the calculation of the derivative is much more complicated than in case of separate (uncoupled) electronic states, but the optimization procedure is the same.

Following the described procedure and starting with the two potentials described in Section 3.3, a minor reduction of the rms of energy differences is achieved (1.17 cm^{-1} in the upper state, down from 1.3 cm^{-1} for the adiabatic potential, but 0.52 cm^{-1} in the lower state, up from 0.3 cm^{-1}). Nevertheless, the shape of the potential is still not satisfactory, because the unphysical oscillation of the lower potential curve close to 5 Å remains (Fig. 4). This work is still in progress. We hope that a proper modelling of the unobserved upper parts of both potentials, which have an influence on perturbation matrix elements, will allow to decrease the rms value and to obtain physically sensible potential curves.

References

[1] MERCIER J.L., RICO R., VELASCO R., *Rotational analysis of some ultraviolet bands of the $^7Li_2$ molecule*, Óptica Pura y Aplicada **2**, 1969, pp. 96–99.

[2] SPIES N., Ph.D. Thesis, Universität Kaiserslautern, Germany, 1990.

[3] THEISS W., MÜSCHENBORN H.J., DEMTRÖDER W., *Laser spectroscopy of the Li$_2$ D$\,^1\Pi_u$ state*, Chemical Physics Letters **174**(2), 1990, pp. 126–132.

[4] DU M., Ph.D. Thesis, Universität Kaiserslautern, Germany, 1996 (cit. after [5]).

[5] WEYH T., LOKAI, DEMTRÖDER W., *Lifetime measurments of the D$\,^1\Pi_u$ state of $^7Li_2$*, Chemical Physics Letters **257**(5–6), 1996, pp. 453–459.

[6] HENN G., Ph.D. Thesis, Universität Kaiserslautern, Germany, 1991 (cit. after [5]).

[7] JASIK P., SIENKIEWICZ J.E., *Calculation of adiabatic potentials of Li$_2$*, Chemical Physics **323**(2–3), 2006, pp. 563–573.

[8] JASIK P., SIENKIEWICZ J.E., *Highly excited electronic states of the lithium dimer*, poster, 41st EGAS, Gdańsk, Poland, 2009.

[9] KUBKOWSKA M.K., GROCHOLA A., JASTRZEBSKI W., KOWALCZYK P., *The C$\,^1\Pi_u$ and 2$\,^1\Sigma_u^+$ states in Li$_2$: experiment and comparison with theory*, Chemical Physics **333**(2–3), 2007, pp. 214–218.

[10] JĘDRZEJEWSKI-SZMEK Z., GROCHOLA A., JASTRZĘBSKI W., KOWALCZYK P., *The 5$^1\Pi_u$ electronic state of the lithium dimer*, Chemical Physics Letters **444**(4–6), 2007, pp. 229–231.

[11] HESSEL M.M., VIDAL C.R., *The B$^1\Pi_u$–X$\,^1\Sigma_g^+$ band system of the $^7Li_2$ molecule*, Journal of Chemical Physics **70**(10), 1979, pp. 4439–4459.

[12] JĘDRZEJEWSKI-SZMEK Z., computer program kalib, http://dimer.fuw.edu.pl/programy/kalib.

[13] FERBER R., JASTRZĘBSKI W., KOWALCZYK P., *Line intensities in V-type polarization labelling spectroscopy of diatomic molecules*, Journal of Quantitative Spectroscopy and Radiative Transfer **58**(1), 1997, pp. 53–60.

[14] PASHOV A., JASTRZĘBSKI W., KOWALCZYK P., *Construction of potential curves for diatomic molecular states by the IPA method*, Computer Physics Communications **128**(3), 2000, pp. 622–634.

[15] LEFEBVRE-BRION H., FIELD R.W., *The Spectra and Dynamics of Diatomic Molecules*, Elsevier, 2004.